

Methods for a quantitative evaluation of odd-even staggering effects

Alessandro Olmi and Silvia Piantelli ^a

Sezione INFN di Firenze, Via G. Sansone 1, I-50019 Sesto Fiorentino (FI), Italy

Received: date / Revised version: date

Abstract. Odd-even effects, also known as *staggering* effects, are a common feature observed in the yield distributions of fragments produced in different types of nuclear reactions. We review old methods, and we propose new ones, for a quantitative estimation of these effects as a function of proton or neutron number of the reaction products. All methods are compared on the basis of Monte Carlo simulations. We find that some are not well suited for the task, the most reliable ones being those based either on a non-linear fit with a properly oscillating function or on a third (or fourth) finite difference approach. In any case, high statistic is of paramount importance to avoid that spurious structures appear just because of statistical fluctuations in the data and of strong correlations among the yields of neighboring fragments.

PACS. 29.85.Fj Data analysis

1 Introduction

An odd-even effect in the yield distributions of final reaction products has been observed since long time in a variety of nuclear reactions. This effect (often called *staggering*) usually consists in an enhanced production of even nuclear species with respect to the neighboring odd ones: for example, in the case of charge distributions, even- Z species are produced more abundantly than the neighboring odd- Z ones¹.

The staggering effect was first investigated long time ago in the fission of actinide nuclei, mainly induced by low-energy neutrons (see e.g. [1, 2, 3, 4, 5, 6] and references therein) and it was attributed to the extra energy required to break a pair of protons or neutrons [7]. Experimentally the odd-even effect in fission was found to be less pronounced for neutrons than for protons. Many investigations were devoted to finding a systematic parametrization of the *normal* shapes, against which experimental results could be compared to extract the odd-even effects. At very low excitation energies, the yield distributions of fission fragments are bell shaped, therefore the normal distributions were assumed to be Gaussians [8]. The odd-even effect appeared as a superimposed saw-tooth modulation.

Having as a reference these semi-empirical shapes, the staggering of low-energy fission was usually quantified by a single value (called *global* staggering) extracted from the whole fragment distribution. Nowadays staggering effects are studied in a variety of different reactions, therefore no

a priori shape of the distribution can be assumed and only *local* values of the staggering can be extracted from small adjacent regions of the yield distributions. An extensive review of different quantitative methods used for estimating local and global average values of the odd-even effects in fission was given by Gönnerwein [9].

For a quantitative analysis, Amiel and Feldstein [10, 11] parametrized the odd-even effects in fission-fragment distributions by assuming that the yields of even- Z fragments are intensified by a factor $(1 + \Delta)$ with respect to the normal distribution and those of odd- Z fragments are reduced by a factor $(1 - \Delta)$, with $\Delta < 1$. The normal behavior is therefore represented by the arithmetic mean between odd and even yield values. The generalization, to take into account odd-even effects as a function of both proton and neutron numbers (usually assumed to be effects independent from each other), leads to the expression

$$Y(Z, N) = Y_{\text{sm}}(Z) (1 \pm \Delta_Z) (1 \pm \Delta_N) \quad (1)$$

where $Y_{\text{sm}}(Z, N)$ is the assumed smooth behavior without staggering; the sign ‘+’ is used for even Z (or N), the sign ‘-’ for odd ones. $\Delta = 0$ if there are no odd-even effects, while $\Delta > 0$ indicates enhanced yields of even species and reduced yields for odd species (vice versa for $\Delta < 0$).

Another approach by Wahl [12] led to a slightly different parametrization

$$Y(Z, N) = Y_{\text{sm}}(Z) (F_Z)^{\pm 1} (F_N)^{\pm 1} \quad (2)$$

$$(F)^{\pm 1} = e^{\pm D}$$

where again the sign ‘+’ is used for even Z (or N) and the sign ‘-’ for odd ones. In this case $F=1$ ($D=0$) corresponds to no odd-even effect, while $F > 1$ ($D > 0$) indicates

^a E-mail: olmi@fi.infn.it, piantelli@fi.infn.it

¹ The opposite effect, i.e. enhancement of odd- Z species and reduction of even ones, is rare and is called *antistaggering*.

enhanced yields for even species and reduced yields for odd species; vice versa for $F < 1$ ($D < 0$). In the parametrization by Wahl, the smooth behavior is represented by the geometric mean between odd and even yield values.

Odd-even effects were discovered also in light complex fragments produced in high-energy fragmentation and spallation reactions [13, 14, 15, 16, 17, 18, 19]. The staggering consisted again in an intensification of the yields of even charges Z with respect to odd ones, although the reaction mechanism, the shape of the charge distributions and the investigated mass region were obviously different from those of low-energy fission experiments.

Recently, staggering effects have been observed also in heavy ion collisions from few MeV/nucleon up to Fermi energies ($15 \leq E/A \leq 50$ MeV/nucleon) [20, 21, 22, 23, 24, 25, 26, 27, 28]. These experiments have stirred renewed interest in staggering phenomena. Indeed, in order to study the symmetry energy [29, 30, 31], one needs to estimate the primary isotopic distributions, which can be reliably reconstructed only if the effects of secondary decays are small or sufficiently well understood.

The staggering has been usually ascribed to nuclear structure effects that manifest in the decay of the excited reaction products or already in the reaction mechanism, if part of the reaction proceeds through low excitation energies [24]. However, in collisions at intermediate energies the preferred interpretation is that the odd-even staggering effect depends – in a complex and presently not very well understood way – on the structure of the nuclei produced near the end of the evaporation chain [17, 23].

Without loss in generality, we will always refer to the charge distributions and to the staggering in charge Z , but of course exactly the same arguments are valid for neutron distributions too. Often the presence of odd-even staggering in Z can be visually appreciated by simple inspection of the charge distributions, especially in regions where the effect is prominent. For regions with reduced staggering, or in the presence of steep variations of the yield as a function of mass or charge, the visualization is more difficult and some specific handling becomes necessary to highlight the existence of staggering effects.

An objective treatment of the data becomes mandatory if one wants to make a quantitative comparison among different experiments or different nuclear systems. Moreover, in contrast with fission fragment studies, for other reaction mechanisms the shape of the yield distribution Y_{sm} has to be deduced from the data with some procedure. The first one, introduced by Tracy et al. [2] in 1972, has been widely used for long time (see, e.g., [17]), but other different treatments have been proposed or can be devised.

In this paper we examine some methods that could be used to put into evidence the presence of the staggering and to quantitatively estimate the magnitude of the phenomenon, without relying on an a priori knowledge of the yield distribution. These methods are briefly described in sect. 2 and the simulation in sect. 3. Section 4 presents the results and a comparison of the different methods.

2 Smoothing methods

When analyzing odd-even effects, the main assumption of eqs. (1) and (2) is that the experimental yield $Y(Z)$ can be factorized into the product of the smooth yield $Y_{\text{sm}}(Z)$ (without staggering effects) multiplied by a staggering factor. In heavy-ion reaction, where $Y_{\text{sm}}(Z)$ is unknown, only a local staggering can be determined. The main, essential assumption is that the staggering varies with Z in a sufficiently *gradual* way to be considered – to a good approximation – *constant* over an interval of a few Z values.

The smoothing procedures used for estimating Δ_Z or D_Z from the data are listed below (each with the corresponding abbreviation that will be used in the paper) and schematically illustrated in figs. 1 and 2. In both figures, the open squares indicate the original cross section without staggering $Y_{\text{sm}}(Z)$, while the open crosses joined by long dashed lines represent what from now on we call the *experimental* cross section $Y(Z)$, because it simulates the outcome of an experiment (for illustration purposes no statistical fluctuations are applied in these two figures). The staggering effects are modelled *à la* Amiel and Feldstein [10, 11], with $\Delta(Z)$ linearly decreasing from 0.12 at $Z=4$ to 0.08 at $Z=9$. The dotted and long dashed lines are just a guide to the eye, joining the points.

1. *Linear interpolation (LIN)*. If the shape of the charge distribution is sufficiently smooth, the simplest estimate of $Y_{\text{sm}}(Z)$ is the average between the original experimental distribution and the same distribution shifted, back and forth, by just one Z unit. This procedure tends to eliminate any periodical oscillation with period $2Z$. Practically, the distribution $\mathcal{Y}(Z)$, which is an estimator of the unknown distribution $Y_{\text{sm}}(Z)$, can be obtained from the experimental one with a linear interpolation:

$$\mathcal{Y}(Z) = [Y(Z-1) + 2Y(Z) + Y(Z+1)] / 4. \quad (3)$$

In fig. 1(a), \mathcal{Y} is estimated by means of the solid line joining the yields $Y_{Z-1/2}$ and $Y_{Z+1/2}$ (open diamonds) obtained by pairwise averaging the experimental data. For each Z , only the measured yields of three consecutive elements (from $Z-1$ to $Z+1$) are needed. The staggering parameter $|\Delta_Z|$ is given by $|Y(Z) - \mathcal{Y}(Z)| / \mathcal{Y}(Z)$ and its effect is indicated by the arrows pointing from the experimental $Y(Z)$ (crosses) to $\mathcal{Y}(Z)$ (full circles). This method is similar to that applied by Zeitlin [16] (and later by others [32, 33]) in high-energy fragmentation studies. Note that in his original version, Zeitlin [16] took as a reference for each given Z the line (dotted in figure) joining $Y(Z-1)$ and $Y(Z+1)$: in this way he obtained a value of Δ_Z exactly twice as large as the present one (open circles).

2. *Interpolation over five points (LIN5)*. In this paper we propose a possible improvement of the previous method by taking into account also the yields of the two neighboring points $Y(Z-2)$ and $Y(Z+2)$. These five yields are pairwise averaged to produce four intermediate values $Y_{Z-3/2}$, $Y_{Z-1/2}$, $Y_{Z+1/2}$ and $Y_{Z+3/2}$

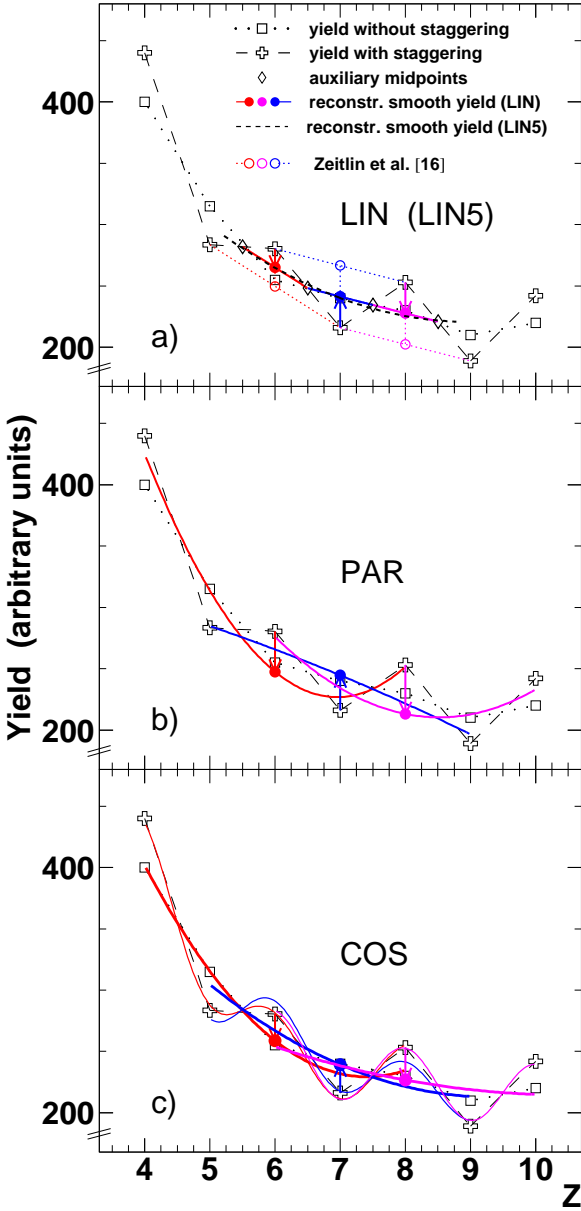


Fig. 1. (color online) Methods (a) LIN and LIN5, (b) PAR and (c) COS. The smooth input distribution (squares) is multiplied (crosses) by the staggering factor $(1 + (-1)^Z \Delta_Z)$. No statistical fluctuations are applied. The thick lines represent the constructions used to estimate the smoothed yield $\mathcal{Y}(Z)$ (full circles), the arrows show the effect of the estimated staggering (see text). Note the ordinate with suppressed origin. For LIN also the method by Zeitlin [16] is shown (open circles).

(open diamonds), which are used to perform a parabolic fit (short dashed line). The value of the fit in the central point Z gives the estimated $\mathcal{Y}(Z)$ and the difference with respect to the measured value is used to estimate Δ_Z .

3. *Parabolic fit (PAR)*. A more refined smoothing method was recently suggested in Ref. [23], based on a fitting procedure too. For each measured value of the yield

$Y(Z)$, the smoothed value $\mathcal{Y}(Z)$ is estimated by fitting a parabolic function,

$$\mathcal{Y}(Z) = a Z^2 + b Z + c, \quad (4)$$

directly to the measured yields over five consecutive values of Z , namely from $Z-2$ to $Z+2$. Figure 1(b) illustrates this method showing three curves, two for the interpolation around even Z (upward parabolas) and the other one around an odd Z (downward parabola). The effect of Δ_Z is again indicated by the arrows pointing from the experimental $Y(Z)$ (crosses) to $\mathcal{Y}(Z)$ (full circles). The three parabolas show the peculiarity of this method. Due to the presence of the staggering, the experimental points have an up-and-down behavior that is obviously not well fitted by a parabola. Therefore, the estimated effect of staggering (arrows in figure) is enhanced. In fact, with respect to the true yields without staggering $Y_{sm}(Z)$ (open squares), the estimated values of $\mathcal{Y}(Z)$ (full circles) lie systematically below for even Z values, and above for odd ones. This has the advantage of amplifying the staggering effect, but at the same time it hinders a proper and quantitative comparison of Δ_Z with the results of other experiments, evaluated with other methods.

4. *Parabolic fit with oscillations (COS)*. In this paper we propose an improvement of the previous method by taking into account the fact that actually, due to staggering, the data oscillate around the assumed smooth behavior. The improvement is accomplished by using a fit function that consists of a parabola multiplied by a properly oscillating function with period $2Z$ and amplitude d_o , like for example

$$\begin{aligned} Y_{fit}(Z) &= (a_o Z^2 + b_o Z + c_o) (1 + d_o \cos(\pi Z)) \\ &= \mathcal{Y}(Z) (1 + d_o \cos(\pi Z)). \end{aligned} \quad (5)$$

At the cost of a non-linear fitting procedure² and by adding a fourth parameter, one obtains a better and more sensible fit (in fact, $Y_{fit}(Z)$ does now take into account the oscillation of the data). There is also an additional bonus: the χ^2 acquires statistical significance and indeed its distribution agrees very well with that expected for the χ^2 function with one degree of freedom. Two variants are possible: (a) deriving Δ_Z from the difference between the estimated $\mathcal{Y}(Z)$ and the measured $Y(Z)$, or (b) directly using the fourth parameter of the fit $\Delta_Z = d_o$. The fits in the five-point intervals around three consecutive Z values are shown by the thin solid lines in fig. 1(c). The thick solid lines show the parabolic part $\mathcal{Y}(Z)$ in eq. (5). The estimate of Δ_Z obtained with variant (a) is indicated once more by the arrows pointing from the experimental $Y(Z)$ (open crosses) to $\mathcal{Y}(Z)$ (full circles). It is apparent that now the circles represent a much better estimate of $Y_{sm}(Z)$ than in the previous method.

² All non-linear fits were performed by means of MINUIT [34] (with successive calls to the routines MIGRAD, HESSE and MINOS) and always reached convergence.

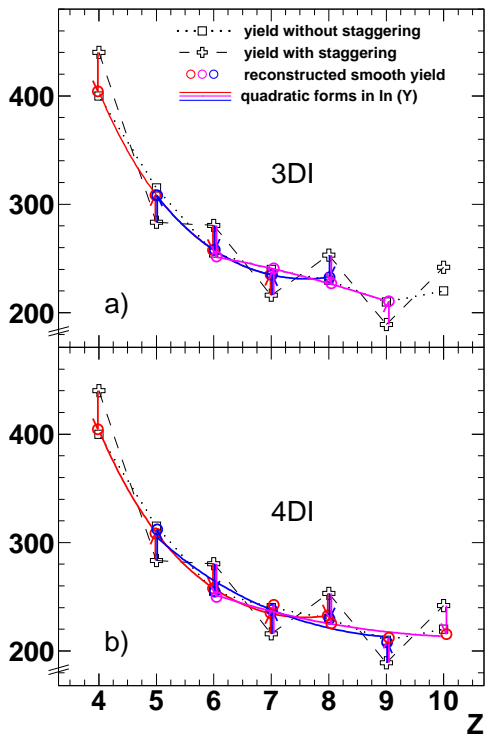


Fig. 2. (color online) Illustration of the methods (a) 3DI and (b) 4DI. Open squares and crosses are the same as in fig. 1. The effect of the estimated staggering is shown by the arrows pointing from the experimental data (crosses) to the reconstructed smooth yields (circles). The full lines correspond to the curves of eq. (7) that best fit the circles. See text for details. Note the expanded vertical scale with suppressed origin.

5. *Third difference method (3DI)*. This is actually the oldest method. First proposed by Tracy [2], it has been widely used in the past and also in recent publications (see e.g. [20,17]). It relies on finite difference calculus and in particular it uses the third difference of the natural logarithm of the measured yield $L(Z) = \ln(Y(Z))$ over four consecutive Z values:

$$D_3(Z + \frac{1}{2}) = \frac{1}{8}(-1)^Z \{L(Z + 2) - 3L(Z + 1) + 3L(Z) - L(Z - 1)\}. \quad (6)$$

The basic assumption is that, without staggering effects, the shape of the logarithm of the yield, $L(Z)$, over the considered interval of four Z values could be described by a parabola

$$L(Z) = a_T Z^2 + b_T Z + c_T. \quad (7)$$

The justification by Tracy was that the smooth behavior of $Y_{sm}(Z)$ over a small interval of Z can be well described by a piece of a Gaussian. It is worth noting that this does *not* necessarily imply that the whole charge distribution needs to be Gaussian-shaped, as it was usually assumed in old-time low-energy fission

studies ³. One can easily verify that with the functional form of eq. (7) (and with no staggering effects) the following identity holds

$$D_3^{ns}(Z + \frac{1}{2}) \equiv 0. \quad (8)$$

If now a fixed quantity D_Z is alternatively added to $L(Z)$ for even Z 's and subtracted for odd ones, then one obtains $D_3(Z + \frac{1}{2}) \equiv D_Z$. One can easily recognize Wahl's parametrization [12] of the staggering with $D_Z \equiv \ln(F_Z)$, see the second eq. (2). The factor $(-1)^Z$ in eq. (6) takes care of the fact that for staggering the sign of D_Z is usually positive for even Z and negative for odd ones. We note also that the result is usually associated with the center of the interval and therefore, being D_3 an *odd* finite difference, that center corresponds to a *half-integer* Z value. An illustration of this method is shown in fig. 2(a), where the arrows pointing from four consecutive experimental values of $Y(Z)$ (crosses) to the corresponding open circles represent the estimated staggering effect over that interval and each solid line is the piece of quadratic polynomial in the logarithm of the yields $L(Z) = \ln(Y(Z))$ that best fits the four circles.

6. *Fourth difference method (4DI)*. Much in line with the method of Tracy [2], in the present paper we propose a new one that considers the fourth central difference over five consecutive points around Z :

$$D_4(Z) = \frac{1}{16} (-1)^Z \{L(Z + 2) - 4L(Z + 1) + 6L(Z) - 4L(Z - 1) + L(Z - 2)\}. \quad (9)$$

Again, the assumption is that without staggering the data are well described by eq. (7) and also in this case one obtains $D_4^{ns}(Z) \equiv 0$. However, if a quantity D_Z is alternatively added to and subtracted from $L(Z)$, one finds again $D_4(Z) \equiv D_Z$. With respect to the previous method, this one uses five points (like all previous methods except LIN and 3DI) and the staggering parameter D_Z can be more physically attributed to the *integer* Z value at the center of the considered interval. An additional advantage of 4DI over 3DI is that eq. (9) remains valid even if $L(Z)$ has some cubic component:

$$L(Z) = a Z^3 + b Z^2 + c Z + d. \quad (10)$$

An illustration of 4DI is shown in fig. 2(b), with the same meaning of symbols and lines as in fig. 2(a).

We point out that the first four methods (LIN, LIN5, PAR, and COS) adopt the staggering parametrization by Amiel and Feldstein [10,11], while the last two are based on that by Wahl [12].

A second dissimilarity is that the first four methods try first to extract from the data the smooth yield $\mathcal{Y}(Z)$ (full circles) that best estimates the unknown $Y_{sm}(Z)$. This in

³ Actually, as either sign is allowed for the coefficient a_T in eq. (7), the shape of $Y(Z)$ is not always a piece of a Gaussian.

turn allows one to determine Δ_Z from the comparison with the experimental yield:

$$\Delta_Z(Z) = (-1)^Z (Y(Z) - \mathcal{Y}(Z)) / \mathcal{Y}(Z) \quad (11)$$

(actually COS gives also Δ_Z directly from the fit). In eq. (11) the factor $(-1)^Z$ takes care again of the opposite signs for even and odd Z values.

On the contrary, in the other two methods (3DI and 4DI) there is generally no need to compute $\mathcal{Y}(Z)$, because eqs. (6) and (9) give directly D_Z , which is the quantity of physical interest. In figs. 2(a) and (b) the underlying $Y_{\text{sm}}(Z)$ distributions have been reconstructed just for illustrative purposes: by subtracting the staggering effect from the experimental yields $Y(Z)$ (crosses), one can deduce the smooth yields (open circles) and draw the curves (solid lines) corresponding to eq. (7).

The two parametrizations by Amiel-Feldstein and Wahl are approximately equivalent in case of small staggering effects ($\Delta_Z \ll 1$), being to first order $D_Z \approx \Delta_Z$. In fact, taking the ratio between the yields for even and odd species in both parametrizations, one obtains the relationship [9]

$$(1 + \Delta_Z)/(1 - \Delta_Z) = (F_Z)^2 \equiv (e^{D_Z})^2 \quad (12)$$

and expanding $1 + 2\Delta_Z + \mathcal{O}(\Delta_Z^2) = 1 + 2D_Z + \mathcal{O}(D_Z^2)$.

In case of larger staggering, a fair quantitative comparison of the results obtained with the two parametrizations may require corrections of higher order [9]:

$$D_Z = \Delta_Z + \frac{1}{3} \Delta_Z^3 + \frac{1}{5} \Delta_Z^5 + \mathcal{O}(\Delta_Z^7) \quad (13)$$

$$\Delta_Z = D_Z - \frac{1}{3} D_Z^3 + \frac{2}{15} D_Z^5 + \mathcal{O}(D_Z^7) \quad (14)$$

3 Simulation

A comparison of the different methods, to find out their possible advantages and disadvantages, is best performed by means of simulations. In this way one can play with the smooth yield distribution $Y_{\text{sm}}(Z)$ and with the parameter Δ_Z , in order to produce a final distribution $Y(Z)$ (including statistical fluctuations) that simulates the experimental one. This allows one to test in how far the different methods are able to retrieve the original $Y_{\text{sm}}(Z)$ and the genuine odd-even effect Δ_Z . In the simulations for the present paper the Amiel and Feldstein parametrization (Δ_Z) has been adopted and the results of the 3DI and 4DI methods (that deliver D_Z) have been transformed by means of eq. (14).

The simulation proceeds in the following steps:

1. A smooth analytic function $f(x)$ is assumed and its evaluation for integer x ($x \in N$) gives the *discretized* smooth charge distribution $Y_{\text{sm}}(Z)$ without staggering.
2. Following the parametrization by Amiel and Feldstein, the charge distribution with staggering is obtained as $Y(Z) = Y_{\text{sm}}(Z) (1 + (-1)^Z \Delta_Z)$, where in principle Δ_Z could even be a slow-varying function of Z .

3. Statistical fluctuations are produced by means of the random number generator RANLUX [35]. In principle they should be Poisson-distributed, but the number of counts $N_c(Z)$ is always sufficiently large that they can be extracted from a Gaussian distribution with $\sigma^2(Z) = N_c(Z)$. Fluctuations are added to the yield of each charge Z , thus producing an experimental charge distribution that simulates the outcome of an experiment.
4. All the described smoothing methods are applied to the experimental distribution to obtain values of Δ_Z as a function of Z .

Steps 3 and 4 are repeated for a preset number of times, which in our case is always 10^4 .

5. The propagation of the fluctuations on the individual yields, including all possible correlations and non-linearities of the methods, produces – for each Z – a distribution of Δ_Z that can be well fitted with a Gaussian. The centroids $\langle \Delta_Z(Z) \rangle$ give the distribution of the average result (over 10^4 distributions) for each method.
6. The results obtained with the different methods are finally plotted and examined in detail.

With reference to the above step 5, we emphasize that our procedure is equivalent (as we have easily verified with the simulation) to adding up all 10^4 replicas and applying the various methods to the summed distribution (which has a huge statistic). The advantage of our procedure is that the widths of the Gaussians, σ_{Δ} , give the uncertainty on Δ_Z – at the 1σ level – expected in the analysis of *one single* experimental distribution. This is exactly the meaning that will be given to the dashed lines in the panels (b) to (h) of fig. 3 and to the error bars in the panels (b) to (h) of figs. 4 to 6.

Our final aim was to compare the behavior of the different methods of sect. 2, in relation to the magnitude of the staggering effect and to the shape of the charge distribution, as well as to assess the robustness of the result with respect to the statistics of the collected data.

For what concerns the last point, to avoid that intrinsic differences among the various analysis methods are obscured by fluctuations, the *relative* errors on the yields should be kept very small. In the simulation, where the fluctuations are just of statistical nature, it is enough to use a reasonably large number of counts $N_c(Z)$ ⁴.

One should be aware that the fluctuations on one Z affect the estimated value of the staggering parameter Δ_Z also for neighboring charges, and this happens in quite a complicated and correlated way that is difficult to estimate without a simulation. In fact, while in a real experiment one can analyze just one single realization of the charge distribution, a big advantage of the simulation is that one can generate a large number of replicas of the same charge distribution (differing from each other only

⁴ In a real experiment this may not suffice, as one has to include other possible uncertainties, if any, that may affect neighboring charges Z in an independent way (e.g. contaminations, identification uncertainties, and so on).

in the random fluctuations) and all correlations are automatically taken into account in the results.

Finally, the simulation allows one to choose freely the shape of $Y_{sm}(Z)$ in order to see the response of the different methods to the shape of the charge distribution, with special attention to its non-linearity regions.

4 Results

The first thing that we checked is that indeed all methods are unbiased, i.e. in absence of staggering they give $\Delta_Z = 0$ within errors. This is shown in fig. 3, where we consider constant charge distributions, without staggering, with a statistic of 200, 500 and 1000 counts per Z unit (first, second and third columns, respectively). In the first row, fig. 3(a), the continuous, dashed and dot-dashed lines show the relative errors $\Delta Y/Y$ obtained by applying the same three sequences of random errors (step 3 of sect. 3) to the above mentioned constant distributions: in fact the structure is the same, the relative errors being reduced just because of the increasing number of counts. The horizontal dashed lines show the $\pm 1\sigma$ error band expected for just one replica and correspond to relative errors $\Delta Y/Y$ of about $\pm 7\%$ for $N_c=200$, down to about $\pm 3\%$ for $N_c=1000$. This means that in one single realization of the charge distribution (i.e. in one measurement), for each measured Z there is still a probability of $\approx 32\%$ that its measured yield lies outside this band.

These relative errors may seem rather small, but they are amplified by all methods used to estimate Δ_Z . In fact propagating these errors from the yields to Δ_Z leads to the $\pm 1\sigma$ band indicated by the horizontal dashed lines in rows (b) to (h) of fig. 3, its width amounting for all methods to about ± 0.04 when $N_c=200$ and ± 0.02 when $N_c=1000$ ⁵.

But this is not the worst part of the story. The impact of these fluctuations on the estimation of Δ_Z is presented in the lower panels of fig. 3, rows from (b) to (h). One clearly sees that taking the average (step 5 of sect. 3) over 10^4 generated replicas, differing only in the fluctuations, gives $\Delta_Z = 0$ with all methods (full dots). However, the correlated propagation of the fluctuations of neighboring charges gives rise to rather large and nonphysical structures (full, dashed and dot-dashed lines), with different and often opposite phases in different realizations: one realization may have a bump where another one has a valley. It is also worth noting that the spurious bumps or valleys depend only on the particular set of random fluctuation, and they appear to be strictly *in phase* for all analysis methods that can be applied.

The main conclusions that can be drawn from fig. 3 are that (a) fluctuations in the charge distribution are amplified by all methods and the values of Δ_Z for neighboring Z become strongly correlated; (b) good statistic (and reduction of other sources of fluctuations) is therefore mandatory for any experiment addressing this topic;

⁵ Similar absolute uncertainties occur also in presence of staggering and cannot be overlooked: for $\Delta_Z = 0.1$ they correspond to an uncertainty of $\approx \pm 40\%$ (20%) for $N_c=200$ (1000).

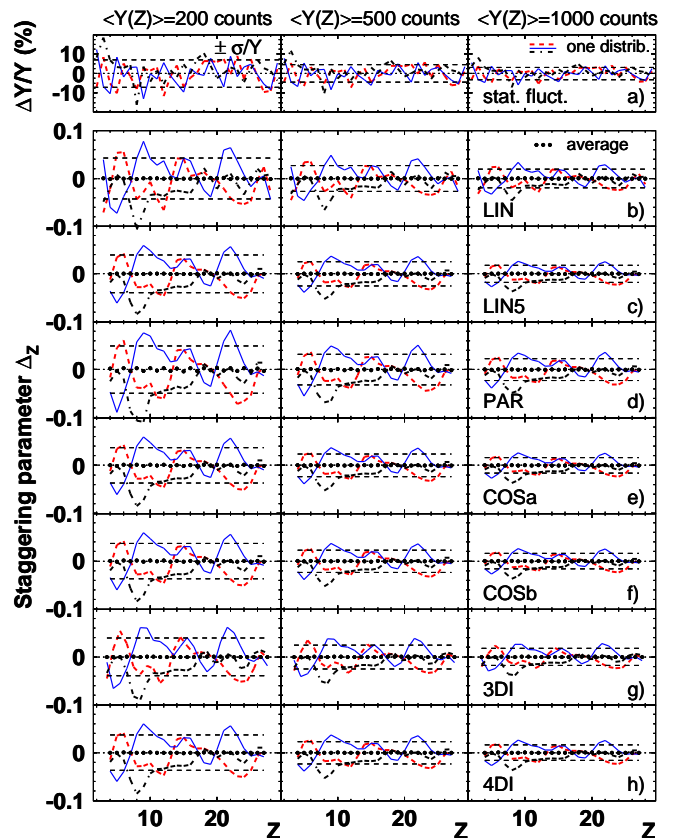


Fig. 3. Effect of statistical fluctuations for three constant charge distributions with 200, 500 and 1000 counts per Z unit (first, second and third column, respectively), without staggering ($\Delta_Z = 0$). Panels in first row (a): relative statistical fluctuations, $(Y - \langle Y \rangle)/\langle Y \rangle$, generated by three different sequences of random numbers (full, dashed and dot-dashed lines), to be applied to the constant distributions to obtain three experimental replicas. Panels in rows from (b) to (h): average values (full dots) of the staggering parameter Δ_Z evaluated over 10^4 distributions with the various methods of this paper, compared with Δ_Z obtained for each of the three replicas (see text).

(c) structures or trends in $\Delta_Z(Z)$ should be interpreted with great caution, after a careful and realistic estimate of their statistical significance.

In the remaining of this paper we will adopt a constant and representative value of $\Delta_Z = 0.1$. In fact we played with possible variations of the staggering magnitude and of its charge dependence, but nothing noteworthy was found. On average (or, equivalently, in a single realization with very small relative errors) almost all methods do an excellent job when the staggering $\Delta_Z = 0.1$ is applied to a charge distribution that either stays constant, or rises or falls in a linear way, whatever the value of its slope. The only exception concerns the method PAR that, with respect to the other methods, amplifies the staggering by about 40% (see Appendix for more details).

Apart the trivial (and unrealistic) case of a linear charge distribution, we now have to investigate how the different

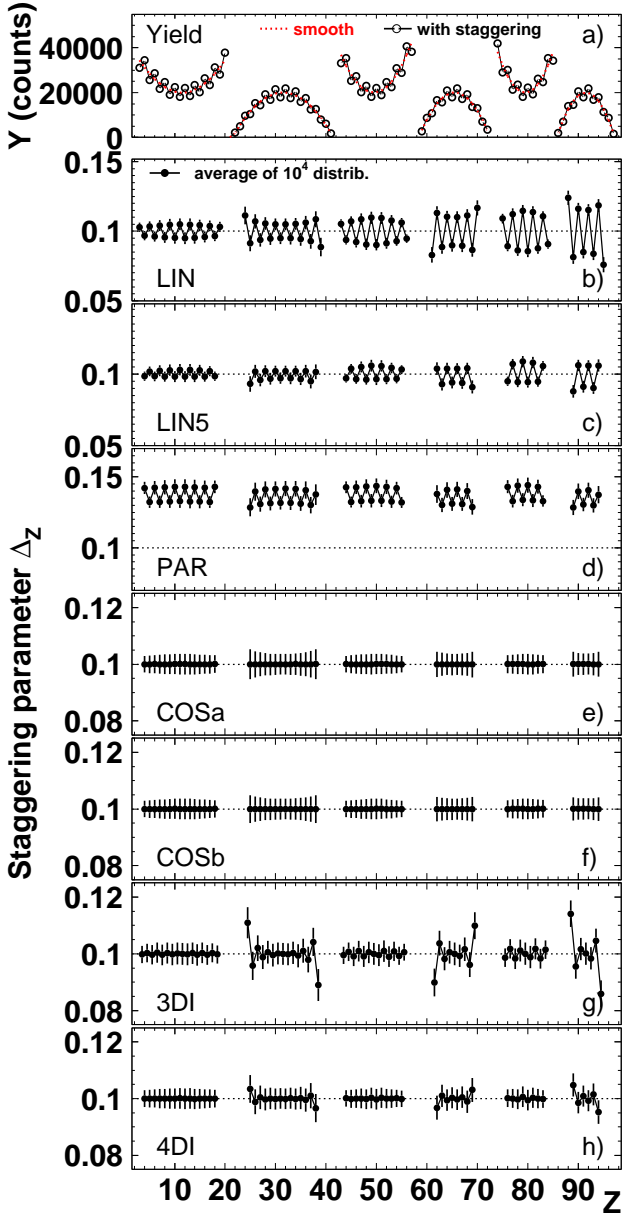


Fig. 4. (color online) Upper panel (a): charge distributions shaped as vertical parabolas (pairwise with the same curvature). Open dots show a constant staggering $\Delta_Z=0.1$ applied to the smooth dashed curves. Panels (b)-(h) present the average $\langle \Delta_Z \rangle$ obtained with the methods LIN, LIN5, PAR, COSa, COSb, 3DI, and 4DI, respectively, compared with the nominal input value (dotted lines). The error bars are the $\pm 1\sigma$ widths of the distributions of Δ_Z . Note that the y-axes for LIN, LIN5 and PAR in panels (b)-(d) span a range twice as large as that of the other methods in panels (e)-(h), while the vertical scale of PAR is shifted upward.

methods behave in regions where the distribution $Y_{sm}(Z)$ is highly not linear (namely it presents an appreciable curvature or has an inflection point) on the basis of some representative cases. Figure 4 shows six examples (three maxima and three minima) of charge distributions shaped as vertical parabolas $y(x) = a(x-x_0)^2 + c$. They have pairwise the same curvature, but with opposite sign ($a = \pm 200$ for the first pair, ± 400 for the second and ± 600 for the third one), while the value in the vertex is always the same, $c = 20000$. With a staggering parameter of $\Delta_Z = 0.1$, the enhancement (reduction) of even (odd) charges Z near the vertex is always the same, namely $+(-)2000$ counts (step 2 of sect. 3).

The lower panels of fig. 4, from (b) to (h), present the result $\langle \Delta_Z \rangle$ obtained with the various methods and averaged over 10^4 replicas of the charge distribution (from now on we will omit the $\langle \rangle$ for simplicity). Note that the vertical scales for the methods LIN, LIN5 and PAR in panels (b)-(d) span a range twice as large as that for the other methods COSa, COSb, 3DI and 4DI in panels (e)-(h). As already anticipated, the error bars represent the statistical uncertainty (at the $\pm 1\sigma$ level) for the analysis of just one replica of the distributions shown in fig. 4(a).

As expected, the simple LIN method, shown in panel (b), is not well suited for distributions with an appreciable curvature and indeed it gives the worst results. The addition of two more points (method LIN5) improves the results, but it makes them acceptable only for the smallest curvatures.

In the PAR method, panel (d), one sees the already mentioned amplification of about 40% and the intrinsic difference between even and odd Z (already reduced by treating the errors as explained in Appendix). The PAR method gives results similar for all curvatures (as expected from the fact that it is based on a parabolic fit), but it does not represent an improvement over LIN5.

For what concerns the remaining methods, they all behave rather well (considering also the amplification by a factor of two of the vertical scale). Of the two methods based on finite difference calculus, 4DI gives some improvement over 3DI, especially for the downward parabolas at the two extremes of the usable Z range (where the statistic is very low), but the best results are definitely obtained by the two new methods, COSa and COSb, which are based on the fit with a properly oscillating function.

The situation is in general even worse for inflection points, which produce more troubles for nearly all methods. In fig. 5(a) we present six charge distributions that differ either in the slope at the inflection point or in the distance between the minimum and the maximum. The distributions are based on cubic functions without quadratic term, $Y(Z) = a(Z-Z_0)^3 + b(Z-Z_0) + c$, all with the same statistic at the inflection point ($c = 20000$). The slope at the inflection point is $b = 1000, 2000$ and 3000 for the first, second and third pair of distributions, respectively, while the cubic coefficient is $a = -50$ for the first and -150 for the second curve of each pair.

The lower panels of fig. 5, from (b) to (h), present the average results for the different methods and again the

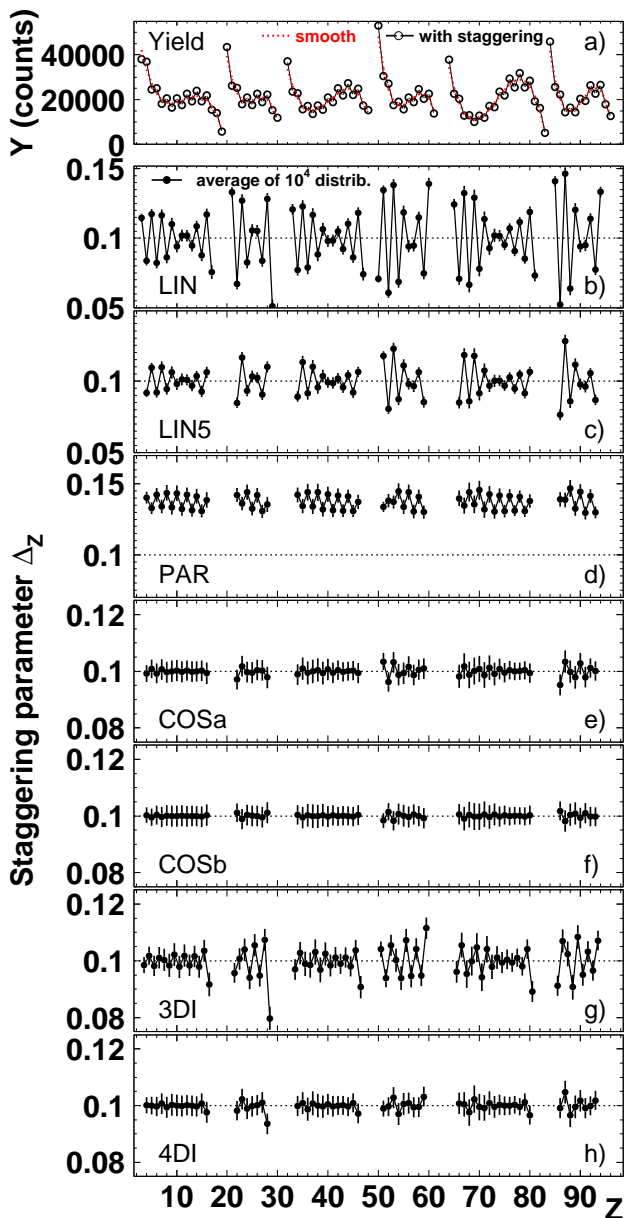


Fig. 5. (color online) Similar to fig. 4, but the upper panel (a) shows charge distributions with different shapes of the inflection points.

vertical scales for the first three methods span a range twice as large as that for the other methods. The method LIN of panel (b) is certainly not acceptable, because it gives systematic deviations up to ± 0.05 with respect to the nominal value of $\Delta_Z = 0.1$. The method LIN5 of panel (c) represents an appreciable improvement, as it cuts down the systematic deviations by about a factor of two. The method PAR of panel (d), in spite of its amplification and systematic even-odd effect, performs better than LIN5.

Of the remaining methods, 4DI of fig. 5(h) is now a very remarkable improvement over the method 3DI by Tracy, shown in panel (g), because it reduces the deviations from the nominal value down to less than ± 0.005 .

The methods COSa and COSb, shown in panels (e) and (f), give results not far from those of 4DI, with the second one, COSb, that definitely gives the best results among all methods displayed in fig. 5.

It is worth noting that the high statistic adopted for the smooth distribution $Y_{sm}(Z)$ (with relative errors lower than $\pm 1\%$ in the non-linear regions) simply makes the presentation of the data in fig. 4 and 5 more readable by reducing the error bars. However, the simulations show that the statistic *does not change* the response of the methods, when it is averaged over 10^4 distributions⁶. Of course, for a single realization (or experiment) a large statistic of the charge distribution remains of paramount importance.

A second point worth noting is that the deviations from the nominal value $\Delta_Z = 0.1$ displayed by some methods in fig. 4 and 5 are characteristic of those methods and of the specific non-linearity of the smooth function Y_{sm} , but do not depend on the chosen value of Δ_Z . In other words, simulations performed with other nominal values of Δ_Z present the same pattern of deviations, with the same absolute magnitude, superimposed on the chosen value of Δ_Z . Therefore, the use of a *good* method with little deviations becomes important especially when the average staggering effect is small. In some cases, this independence of the observed deviations from the nominal Δ_Z can be demonstrated not only with a simulation, but also with a little algebra. For example, if in LIN we assume that near a certain Z the distribution is not linear, but has some additional quadratic component, $Y(Z) = aZ^2 + bZ + c + (-1)^Z \Delta_Z$, then eq. (3) gives $\mathcal{Y}(Z) = Y_{sm}(Z) + a/2$ (instead of $Y_{sm}(Z)$), thus making a bias in eq. (11) that is independent of Δ_Z . And for the method 3DI, if eq. (7) has also some cubic component $L(Z) = dZ^3 + a_T Z^2 + b_T Z + c_T$, then eq. (6) would deliver $D_Z + 6d$ (instead of D_Z), with a bias that again does not depend on the particular value of D_Z .

We used several other shapes of the charge distribution, finding that in all cases, irrespective of the specific shape, the ranking of the various methods remains similar to that shown by figs. 4 and 5.

Therefore we show just one case in fig. 6, where a more realistic charge distribution, open dots in panels (a), mimics the typical features found in semi-peripheral collisions of intermediate-energy heavy-ion reactions: with increasing Z there is a very rapid drop of the cross section from the lightest complex fragments with $Z \approx 4$ down to a wide valley of intermediate mass fragments (IMF) around $Z \approx 10 - 15$, followed by a slow rise towards heavier ones (which may represent either fission-like or projectile-like fragments) that finally fades away.

This shape was obtained with a *natural cubic spline* passing through seven equally spaced knots (the five internal ones are indicated by thin vertical lines in the figure): it is a piece-wise interpolation with 3rd degree polynomials that is continuous in the joining knots up to the second

⁶ For example, one sees from eqs. (3), (11) that a common factor k multiplying all yields cancels out in the average $\langle \Delta_Z \rangle$; and it cancels out also in $\langle D \rangle$, when $\langle \ln(kY) \rangle = \ln(k) + \ln(\prod_{i=1}^N Y_i)/N = \ln(k) + \langle \ln(Y) \rangle$ is inserted in eqs. (6) or (9).

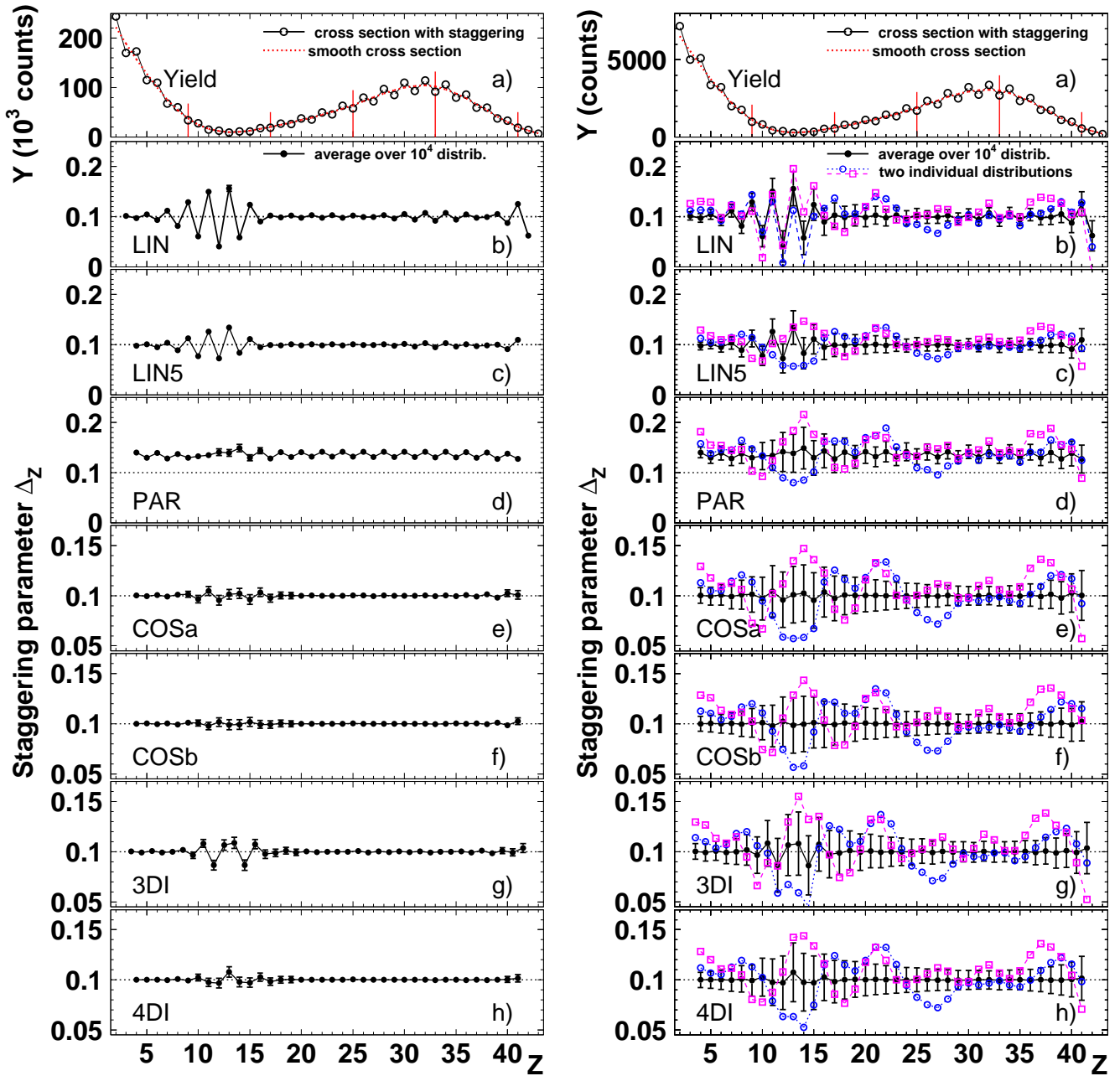


Fig. 6. (color online) Upper panels (a): charge distributions based on the same *natural cubic spline* (smooth dashed line); the thin vertical lines indicate the internal knots (see text). The left part shows a distribution with high statistic, the right part the same with low statistic. Open dots display the effect of a constant staggering $\Delta_z = 0.1$. Panels (b)-(h) present Δ_z obtained with the methods LIN, LIN5, PAR, COSa, COSb, 3DI, and 4DI, respectively, compared with the nominal value of 0.1 (dotted lines). For each Z , the error bar indicates the width ($\pm 1\sigma$) of the distribution of Δ_z obtained from 10^4 simulations. The y-axes for LIN, LIN5 and PAR span a range twice as large as that of the other methods in panels (e)-(h). The average behavior over 10^4 realizations (full dots) is the same in the left and right parts of the figure, only the fluctuations (error bars) expected for a single realization obviously differ very much. In the left panels (b)-(h), the open dots/squares (joined by dashed/dotted lines) present the correlated propagation of the statistical fluctuations for two single realizations of the low-statistic charge distribution.

derivative. The adjective *natural* indicates the additional conditions that the second derivative is zero in the two external knots. The statistic for each one of the 10^4 generated replicas is very large in the left part of the figure (in the IMF valley it corresponds to at least ten thousand counts for each charge Z) and very low in the right part (about 300 counts per charge Z in the IMF valley).

The lower panels, from (b) to (h), illustrate again the estimates of Δ_Z obtained with the various methods LIN, LIN5, PAR, COSa, COSb, 3DI, and 4DI, respectively. The full dots represent the average obtained over 10^4 simulations, while the hardly visible error bars give the widths of the distributions for each Z . Again the dashed lines at $\Delta_Z = 0.1$ indicate its nominal value. For the methods LIN, LIN5 and PAR the vertical scale spans a range about a factor of two wider than for the other methods.

Also in this case we observe an evident failure of LIN and LIN5 in the minimum of the IMF valley and in the final tail of the distribution. Of the two finite-difference methods the new one, 4DI performs better, but the best results are obtained with the fitting methods COS and particularly with the second one, COSb.

In the right part of the figure, the average behavior is the same as in the left part, only the $\pm 1\sigma$ fluctuations (error bars) expected for a single realization (or measurement) are much larger. Two examples of the results obtained for two individual random realizations of the charge distribution are shown by the open dots/squares, joined by dashed/dotted lines in the panels (b)-(h) of the right part of the figure. Here the effects of the statistical fluctuations are clearly visible with all methods and reveal marked deviations from the average behavior, with several points located outside the error bars. What is even worse is the fact that the fluctuations give rise to structures involving several neighboring points, a consequence of their correlation (see next section). The location and the amplitude of these nonphysical structures present large random variations from one single realization to the other, being sometimes in-phase and sometimes out-of-phase in the two realizations. This means that in a single experiment, unless the statistic is very large and the independent relative errors very small (below the 1% level), the physical significance of structures in the staggering parameter Δ_Z should be treated with great caution.

5 Correlations

The need of estimating the smooth behavior of the charge distribution from a few data points, naturally introduces short-range autocorrelations among the staggering parameters Δ_Z pertaining to neighboring charges Z . The degree of autocorrelation is estimated with the usual definition

$$R(Z', Z'') = \frac{\langle (\overline{\Delta_{Z'}} - \overline{\Delta_{Z'}}) (\overline{\Delta_{Z''}} - \overline{\Delta_{Z''}}) \rangle}{\sigma_{\Delta_{Z'}} \sigma_{\Delta_{Z''}}} \quad (15)$$

where the overlined $\overline{\Delta_Z}$'s are the mean values of the staggering parameters for two different charges Z' and Z'' , the brackets $\langle \rangle$ indicate the expectation value of the product

of the deviations of the two Δ_Z from their mean values and the σ 's in the denominator are their standard deviations. By construction $R(Z', Z'')$ lies in the range $[-1, 1]$, the two extremes indicating perfect correlation or anticorrelation, respectively (while 0 indicates uncorrelated data).

The correlation factor R cannot be estimated from a single experiment, but it is easily obtained in a simulation where many replicas of a certain charge distribution are generated, differing only in the fluctuations. As expected, fluctuations introduce a correlation that is positive for two nearby located Z' and Z'' values and 0 for distant ones.

The correlation factor is practically independent of the specific shape of the analyzed charge distributions. For a flat distribution with a constant Δ_Z of 0.1, the region of positively correlated neighboring Z values is obviously five charge units wide for the methods LIN5, PAR, COS and 4DI (with a common FWHM of 3.24 ± 0.03) and decreases to four and three charge units for the methods 3DI and LIN (with FWHM values of 2.84 and 2.37, respectively). In conclusion, structures possibly found in the staggering analysis that are narrower than the above numbers are highly suspicious and probably they should not be given any physical significance.

6 Conclusions

The odd-even staggering is a widespread phenomenon that usually consists in a relative enhancement of the yields of nuclei with even values of proton (neutron) number Z (N) with respect to the neighboring nuclei with odd values. All methods are based on the idea, first proposed by Amiel and Feldstein [10,11], that the measured yield $Y(Z)$ can be factorized into the product of a smooth yield $Y_{sm}(Z)$ times a factor $(1 \pm \Delta_Z)$, where the sign '+' holds for even charges and the sign '-' for odd ones.

This is an assumption, widely accepted and probably justifiable on the basis of theoretical arguments, but it remains an assumption and one should definitely remain aware of that.

We have revised some old methods and we propose some new methods of extracting the staggering parameter Δ_Z from the experimental charge distributions. Some methods first estimate the underlying smooth behavior of the yield $\mathcal{Y}(Z)$ from the data themselves, and then they derive the staggering from the difference between the measurement and the smoothed yield, while others deliver a direct estimate of the staggering parameter.

Almost all methods perform equally well if the charge distribution has a predominant linear behavior, while they greatly differ from each other in the presence of strongly non-linear regions in the charge distribution. All methods are extremely sensitive to the fluctuations that may affect the yields of neighboring Z in the experimental data, giving origin to spurious structures without much physical meaning. Therefore for this kind of studies it is of paramount importance to acquire good data with very large statistic and very small independent relative errors, so that the relative random fluctuations for each measured Z are of the order of about 1% or better: only in such a

case one can appreciate the different quality of the various methods. On the contrary, if the fluctuations are appreciably larger, spurious effects appear, and it makes no much sense to choose one method rather than another; the results will be anyhow poor and hard to interpret in a sensible way.

We find that a linear interpolation (LIN) between three neighboring points gives the worst results among all examined methods. A linear interpolation over five points (LIN5) brings only some moderate improvement. The recently proposed fit of a simple parabola over five points (PAR) presents the peculiarity that it amplifies the signal, but it needs a careful treatment of the errors and even then it does not produce a really smooth estimate of the distribution without staggering $\mathcal{Y}(Z)$.

Very good results are given by the newly proposed method (COS) that uses a five-point fit with a properly oscillating function. As it implies a non-linear fit, a reliable recursive procedure has to be used, such as the well known MINUIT code [34] developed in CERN. Using directly the coefficient of the oscillating term (method COSb) as delivered by the fit seems to be the best way to estimate the staggering parameter Δ_Z .

A completely different approach is the oldest one by Tracy, based on the third (3DI) finite differences over four points. At variance with the previous methods, it delivers directly an estimate of the staggering parameter, although with a slightly different parametrization first proposed by Wahl [12]. The staggering value that is usually attributed to the center of the considered interval in this case corresponds to a half-integer Z . This method gives good results, better than the LIN, LIN5 and PAR methods, but not as good as the COSb method.

The new method proposed in this paper (4DI) is similar to 3DI, but uses the fourth finite differences over five points. It gives somewhat better results than the original 3DI because it is insensitive to possible cubic components in the smooth charge distribution, and probably also because it uses one more point and hence it is slightly less sensitive to fluctuations. Moreover, one practical (and aesthetic) advantage is that the result can be attributed to the integer Z value at the center of the five-point interval. Based on our analysis it represents the second choice after the COSb method.

Concluding, to avoid the appearance in $\Delta_Z(Z)$ of structures without much physical significance i) one should collect data with a very large statistic; ii) all other uncertainties that may affect the yields of neighboring Z in an independent way should also be carefully estimated and reduced; iii) once the previous conditions are met, the method which is less sensitive to non-linearities of the underlying smooth distribution $Y_{sm}(Z)$ is the method COSb, closely followed by the method 4DI.

Appendix

With respect to the others, the method PAR amplifies the estimated Δ_Z by about 40% above the nominal value. This fact may be viewed as an advantage, but in any case it has

to be taken into account when quantitatively comparing the results of this method with those of the others. A second characteristic intrinsic in the PAR method is that this amplification is not the same for even and odd charges. It is somewhat larger for even charges (that are usually enhanced by staggering) than for odd ones, so that even in case of constant input values of the yield $Y_{sm}(Z)$ and of the parameter Δ_Z , one does not obtain a really flat Δ_Z distribution, even for an input value of $\Delta_Z=0$ (see full dots in panels of row (d) in fig. 3).

This effect is connected with the weights used in the *weighted least squares fit* procedure. When the smoothed yield $\mathcal{Y}(Z)$ is deduced by means of a fit (like in the PAR and COS methods), some care must be put in the treatment of the errors on the measured yields $Y(Z)$. In fact the *weighted least square fit method* may introduce a subtle asymmetry between even and odd Z values when the weights depend on the number of counts measured for each Z . In this case, even Z yields (which are enhanced) have systematically somewhat larger errors (and hence smaller weights) than odd Z yields.

This causes an artifact in the PAR method because the parabola is not the appropriate function to fit the five ‘zigzagging’ experimental points. This is shown in fig. 7(a), where a constant yield of 1000 counts with $\Delta_Z=0.1$ is assumed, leading to statistical weights of about $1/\sqrt{1100}$ and $1/\sqrt{900}$ for the even and odd Z , respectively. With

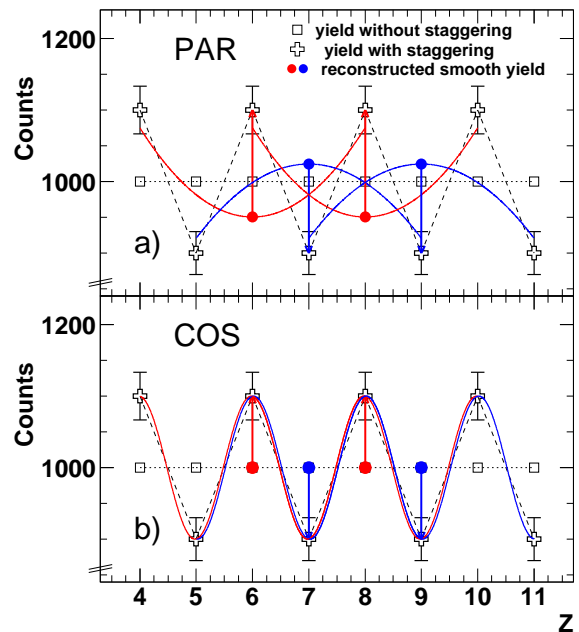


Fig. 7. (color online) Effect of applying a *weighted least square fit* in the PAR (a) and COS (b) methods, with the weights taken from the statistics of the data. The original distribution (squares) is flat with a statistic of 1000 counts; a $\Delta_Z=0.1$ staggering effect (crosses) is superimposed on it. In the PAR method the differing statistical errors for even and odd Z induce an artifact that estimates a larger staggering for even Z than for odd ones (see text).

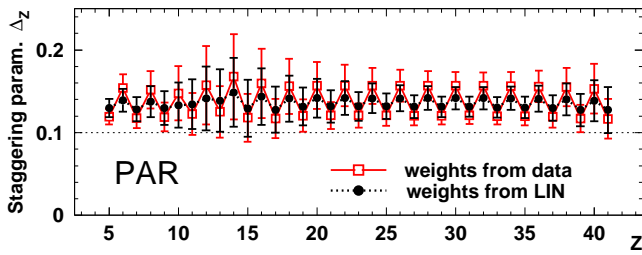


Fig. 8. (color online) Staggering parameter Δ_Z for the charge distribution on the right part of fig. 6(a) obtained with the method PAR using the *weighted least square fit* with statistical errors estimated directly from the experimental data (open squares), or by first applying the LIN method (full dots).

their larger weights, the three reduced yields (lower crosses) of an odd Z are more effective in shifting the parabola downward than the three enhanced yields (upper crosses) of an even Z in shifting it upward, due to their smaller weights: as a consequence, even Z values appear to have a larger staggering than odd ones. We stress that this effect *cannot* be cured by increasing the statistic of the measurement, as long as the errors depend on the statistic. It is worth noting that, on the contrary, the fits of the COS method shown in fig. 7(b) are not affected by this problem, because this method uses a properly oscillating fit function that well reproduces the data.

The open squares of fig. 8 show the effect on Δ_Z when the errors in PAR are estimated directly from the data, in case of the charge distribution already presented in the right part of fig. 6(a). This artifact may be cured either by recurring to the *unweighted least square method* (which is however unsatisfactory when the yields strongly vary with Z) or performing appropriate averages of the weights before fitting the data. In this paper we always used as statistical weights for the PAR method the results of a preceding analysis performed with the LIN method. This artifice proved essential to obtain results (full dots in fig. 8) that could be meaningfully compared with the other methods.

We wish to warmly thank Prof. P.R. Maurenzig for continuous support and very fruitful discussions.

References

- N. G. Runnalls, D. E. Troutner, and Robert L. Ferguson, Phys. Rev., 179 (1969) 1188.
- B. L. Tracy, J. Chaumont, R. Klapisch, J. M. Nitschke, A. M. Poskanzer, E. Roeckl, and C. Thibault, Phys. Rev. C **5** (1972) 222.
- H.-G. Clerc, W. Lang, H. Wohlfarth, K.-H. Schmidt, H. Schrader, K. E. Pferdekämper, and R. Jungmann, Z. Phys. **A274** (1975) 203.
- G. Siegert, H. Wollnik, J. Greif, R. Decker, G. Fiedler, and B. Pfeiffer, Phys. Rev. C **14** (1976) 1864.
- K.-H. Schmidt, J. Benlliure, and A. R. Junghans, Nucl. Phys. **A693** (2001) 169.
- I. Tsekhanovich, N. Varapai, V. Rubchenya, D. Rochman, G. S. Simpson, V. Sokolov, G. Fioni, and Ilham Al Mahamid, Phys. Rev. C **70** (2004) 044610.
- F. Rejmund, A. V. Ignatyuk, A. R. Junghans, and K.-H. Schmidt, Nucl. Phys. **A678** (2000) 215.
- A. C. Wahl, R. L. Ferguson, D. R. Nethaway, D. E. Troutner, and K. Wolfsberg, Phys. Rev. **126** (1962) 1112.
- F. Gönnewein, Nucl. Instrum. Methods **A316** (1992) 405.
- S. Amiel and H. Feldstein, In *Third International Symposium on Physics and Chemistry of Fission*, volume II, page 65. IAEA, Vienna (1974).
- S. Amiel and H. Feldstein, Phys. Rev. C **11** (1975) 845.
- A. C. Wahl, J. Radioanalytical Chemistry, **55** (1980) 111.
- A. M. Poskanzer, G. W. Butler, and E. K. Hyde, Phys. Rev. C **3** (1971) 882.
- W. R. Webber, J. C. Kish, and D. A. Schrier, Phys. Rev. C **41** (1990) 533.
- C. N. Knott, S. Albergo, Z. Caccia, C.-X. Chen, S. Costa, H. J. Crawford, M. Cronqvist, J. Engelage, P. Ferrando, R. Fonte *et al.*, Phys. Rev. C **53** (1996) 347.
- C. Zeitlin, L. Heilbronn, J. Miller, S. E. Rademacher, T. Borak, T. R. Carter, K. A. Frankel, W. Schimmerling, and C. E. Stronach, Phys. Rev. C **56** (1997) 388.
- M. V. Ricciardi, A. V. Ignatyuk, A. Kelič, P. Napolitani, F. Rejmund, K.-H. Schmidt, and O. Yordanov, Nucl. Phys. **A733** (2004) 299.
- P. Napolitani, K.-H. Schmidt, L. Tassan-Got, P. Armbruster, T. Enqvist, A. Heinz, V. Henzl, D. Henzlova, A. Kelič, R. Pleskač *et al.*, Phys. Rev. C **76** (2007) 064609.
- P. Napolitani, K.-H. Schmidt, and L. Tassan-Got, J. Phys. G **38** (2011) 115006.
- L. B. Yang, E. Norbeck, W. A. Friedman, O. Bjarki, F. D. Ingram, R. A. Lacey, D. J. Magestro, M. L. Miller, A. Nadasen, and R. Pak *et al.*, Phys. Rev. C **60** (1999) 041602.
- E. M. Winchester, J. A. Winger, R. Laforest, E. Martin, E. Ramakrishnan, D. J. Rowland, A. Ruangma, S. J. Yenello, G. D. Westfall, A. Vander Molen, and E. Norbeck, Phys. Rev. C **63** (2000) 014601.
- E. Geraci, M. Bruno, M. D'Agostino, E. De Filippo, A. Pagano, G. Vannini, M. Alderighi, A. Anzalone, L. Auditore *et al.*, Nucl. Phys. **A732** (2004) 173.
- M. D'Agostino, M. Bruno, F. Gulminelli, L. Morelli, G. Baiocco, L. Bardelli, S. Barlini, F. Cannata, G. Casini, E. Geraci *et al.*, Nucl. Phys. **A861** (2011) 47.
- G. Ademard, J. P. Wieleczo, J. Gomez del Campo, M. La Commara, E. Bonnet, M. Vigilante, A. Chbihi, J. D. Frankland, E. Rosato, G. Spadaccini *et al.*, Phys. Rev. C **83** (2011) 054619.
- I. Lombardo, C. Agodi, F. Amorini, A. Anzalone, L. Auditore, I. Berceanu, G. Cardella, S. Cavallaro, M. B. Chatterjee, E. De Filippo *et al.*, Phys. Rev. C **84** (2011) 024613.
- M. D'Agostino, M. Bruno, F. Gulminelli, L. Morelli, G. Baiocco, L. Bardelli, S. Barlini, F. Cannata, G. Casini, E. Geraci *et al.*, Nucl. Phys. **A875** (2012) 139.
- G. Casini, S. Piantelli, P. R. Maurenzig, A. Olmi, L. Bardelli, S. Barlini, M. Benelli, M. Bini, M. Calviani, P. Marini *et al.*, Phys. Rev. C **86** (2012) 011602(R).

28. S. Piantelli, G. Casini, P. R. Maurenzig, A. Olmi, S. Barlini, M. Bini, S. Carboni, G. Pasquali, G. Poggi, A. A. Stefanini, S. Valdrè *et al.*, *Phys. Rev. C* **88** (2013) 064607.
29. M. Colonna and F. Matera, *Phys. Rev. C* **71** (2005) 064605.
30. Ad. R. Raduta and F. Gulminelli, *Phys. Rev. C* **75** (2007) 044605.
31. Jun Su, Feng-Shou Zhang, and Bao-An Bian, *Phys. Rev. C* **83** (2011) 014608.
32. G. Iancu, F. Flesch, and W. Heinrich, *Radiat. Meas.* **39** (2005) 525.
33. J. X. Cheng, X. Jiang, S. W. Yan, and D. H. Zhang, *J. Phys. G* **39** (2012) 055104.
34. F. James. "MINUIT: Function Minimization and Error Analysis - Reference Manual", <http://wwwasdoc.web.cern.ch/wwwasdoc/minuit/minmain.html> (2000).
35. M. Luescher. "A portable high-quality random number generator for lattice field theory calculations", *Computer Physics Communications* **79** (1994).